Bifurcation threshold of the delayed van der Pol oscillator under stochastic modulation

Mathieu Gaudreault[1], François Drolet[1,2], and Jorge Viñals[3]

[1] *Department of Physics, McGill University, Montréal, Québec, Canada, H3A 2T8.* [2] *FPInnovations, 570 Saint-Jean Blvd., Pointe Claire, Québec, Canada, H9R 3J9.* [3] *School of Physics and Astronomy, and Minnesota Supercomputing Institute, University of Minnesota, Minneapolis, Minnesota 55455.*

(Dated: March 31, 2011)

Abstract

We obtain the location of the Hopf bifurcation threshold for a modified van der Pol oscillator, parametrically driven by a stochastic source and including delayed feedback in both position and velocity. We introduce a multiple scale expansion near threshold and solve the resulting Fokker-Planck equation associated with the evolution at the slowest time scale. We also verify the asymptotic results by direct numerical integration of the governing equation. We show that the stochastic bifurcation threshold is shifted relative to the deterministic limit by an amount that scales with the amplitude of the feedback terms in the model.

PACS numbers: 02.30.Ks, 05.10.Gg, 05.70.Ln, 87.16.Yc, 87.18.Cf

I. INTRODUCTION

The deterministic van der Pol oscillator was introduced by Appleton and van der Pol to describe triode oscillations in electrical circuits [1]. Since then, the model has been used as a prototypical equation that describe self-excited stable oscillations. One class of recent extensions of the model involve delayed feedback and its effect on the stability of the limit cycle.

The van der Pol model supplemented with delayed feedback plays an important role in the theory of nonlinear vibration. For example, complex response due to time delay such as bifurcation, high amplitude vibration, or quasi-periodic motion or chaotic behavior may cause the failure of an engineered structure subjected to vibration due to its environment. On the other hand, careful choices of parameters may enhance the control of oscillatory systems. For instance, it has been shown in a periodically driven van der Pol oscillator with delay terms in position and velocity, that feedback may control the amplitude of oscillation and even suppress quasi-periodic motion [2–4]. A similar model but with a cubic nonlinearity has been investigated via a center manifold reduction together with an averaging method [5] to show that time delay can act as an effective switch, and control motion either from regular motion to a chaotic behavior or vice versa. The dynamics of a forced van der Pol-Duffing with both linear and nonlinear feedback control has also been studied [6, 7] as an example of a Neimark-Sacker bifurcation to quasi periodic motion.

The bifurcation diagram of the van der Pol oscillator without delayed feedback but parametrically driven by a stochastic source is well known. It has been obtained by either a perturbation analysis of the linear stability problem [8], or by adiabatic reduction [9]. It is found that the bifurcation point is shifted relative to the deterministic limit by an amount that is proportional to the intensity of the randomness. This model has also been investigated by using a multiple scales expansion of the solution in order to derive the resulting slow amplitude or envelope equations near the bifurcation [10–13]. The same multiple scale method has been used to analyze stochastic differential equations with delayed feedback in order to derive the stochastic time evolution of the envelope of the oscillation [14, 15] as well as to determine the location of the bifurcation threshold if the time delay is small [16]. Our focus here is an extension of this latter work, and focuses on a nonlinear oscillator with delayed feedback that is stochastically driven. We pay especial attention to the interplay

between the delayed feedback and temporal correlations, and its effect on the stability of oscillation.

We present in this paper an analytical determination of the bifurcation threshold of the van der Pol oscillator under stochastic parametric driving and delayed feedback by a multiple scale expansion method. We find that the threshold is shifted relative to the deterministic limit by an amount that scales linearly with the time delay and the intensity of the stochasticity. The method also allows the determination of the Hopf frequency close to the bifurcation.

II. BIFURCATION DIAGRAM OF THE VAN DER POL OSCILLATOR

Consider an extension of the classical van der Pol oscillator [17] that includes delayed feedback in position and velocity of the oscillator,

$$\ddot{x}(t) + \omega_0^2 x(t) + \eta x(t-\tau) = \beta\dot{x}(t) + \kappa\dot{x}(t-\tau) - bx^2(t)\dot{x}(t) + x(t)\xi(t) \;, \tag{1}$$

where ω_0, η, β, κ, and b are constants of order $O(1)$, $\tau > 0$ is the time delay, and $\xi(t)$ is a Gaussian white noise with zero mean $\langle \xi(t) \rangle = 0$ and variance $\langle \xi(t)\xi(t') \rangle = 2D\delta(t-t')$, where D is the intensity of the randomness.

In the deterministic limit of $D = 0$, and without delayed feedback ($\eta = \kappa = 0$), the oscillator has a fixed point at $(x, \dot{x}) = (0, 0)$ [18]. The stability of this fixed point is determined by the eigenvalues $\lambda = \beta(1 \pm \sqrt{1 - 4\omega_0^2/\beta^2})/2$. If $\beta < 0$, the fixed point is stable. Otherwise, the fixed point is unstable and the trajectory is a periodic orbit. The Hopf bifurcation is located at the point where the eigenvalue is zero, which occurs at $\beta = 0$.

We next proceed to determine the bifurcation diagram of the full model (1). We begin by introducing a multiple scale expansion method to determine the asymptotic evolution of Eq. (1) near threshold. We assume that there are two dominant time scales near threshold: oscillations that evolve over a fast time scale t and a slow envelope that evolves over a slower time scale $T = \epsilon^2 t$, where $\epsilon > 0$ is a small number. Random contributions that are faster than the oscillation frequency are assumed to average away. We introduce the solutions,

$$x(t, T) \;=\; \epsilon A(T)\cos(\omega t) - \epsilon B(T)\sin(\omega t) \;, \tag{2}$$

$$\dot{x}(t, T) \;=\; -\epsilon\omega A(T)\sin(\omega t) - \epsilon\omega B(T)\cos(\omega t) \;, \tag{3}$$

where ω is the frequency of the fast oscillation. The Stratonovich and Ito interpretations of Eq. (1) are in the case of this equation equivalent. We choose however the Stratonovich interpretation. Change of variables follows the rules of ordinary calculus under this interpretation [19]. Hence, substitute Eqs. (2) and (3) into Eq. (1) by using $\partial_t \to \partial_t + \epsilon^2 \partial_T$,

$$\begin{aligned}
\epsilon^3 \partial_T A(T) \sin(\omega t) + \epsilon^3 \partial_T B(T) \cos(\omega t) = -\frac{1}{\omega} \{ & \\
& (\omega^2 - \omega_0^2) \left[\epsilon A(T) \cos(\omega t) - \epsilon B(T) \sin(\omega t) \right] \\
& - \eta \left[\epsilon A(T - \epsilon^2 \tau) \cos[\omega(t-\tau)] - \epsilon B(T - \epsilon^2 \tau) \sin[\omega(t-\tau)] \right] \\
& - \beta\omega \left[\epsilon A(T) \sin(\omega t) + \epsilon B(T) \cos(\omega t) \right] \\
& - \kappa\omega \left[\epsilon A(T - \epsilon^2 \tau) \sin[\omega(t-\tau)] + \epsilon B(T - \epsilon^2 \tau) \cos[\omega(t-\tau)] \right] \\
& + b\omega \left[\epsilon A(T) \cos(\omega t) - \epsilon B(T) \sin(\omega t) \right]^2 \left[\epsilon A(T) \sin(\omega t) + \epsilon B(T) \cos(\omega t) \right] \\
& + \left[\epsilon A(T) \cos(\omega t) - \epsilon B(T) \sin(\omega t) \right] \xi(t) \} \, .
\end{aligned} \tag{4}$$

The original time delay τ is finite, and hence small in the slow time scale T. Hence we have $A(T - \epsilon^2 \tau) \approx A(T)$ and $B(T - \epsilon^2 \tau) \approx B(T)$. Define also the parameters $\mu = \beta\omega + \eta \sin(\omega\tau) + \omega\kappa \cos(\omega\tau)$ and $\nu = \omega^2 - \omega_0^2 - \eta \cos(\omega\tau) + \omega\kappa \sin(\omega\tau)$ for simplicity.

We next average out the dependence on the fast time scale by integrating over a period of oscillation. Multiply both sides of Eq. (4) by $L^{-1} \int_0^L dt \sin(\omega t)$, where $L = 2\pi/\omega$ and perform the integration. We obtain a stochastic differential equation describing the dynamics of the envelope variable $A(T)$ over the slow time scale,

$$\begin{aligned}
\epsilon^3 \partial_T A(T) = \frac{1}{\omega} \Bigg\{ & \mu \epsilon A(T) + \nu \epsilon B(T) - \epsilon^3 \frac{b\omega}{4} A(T) \left[A^2(T) + B^2(T) \right] \\
& + \epsilon B(T) \frac{1}{L} \int_0^L \xi(t) dt - \epsilon B(T) \frac{1}{L} \int_0^L \cos(2\omega t) \xi(t) dt - \epsilon A(T) \frac{1}{L} \int_0^L \sin(2\omega t) \xi(t) dt \Bigg\} \, .
\end{aligned} \tag{5}$$

The stochastic integrals need to be transformed to the slow time scale. We first use the relation $T = \epsilon^2 t$ to write

$$\xi(t) = \epsilon \xi_0(T) \, , \tag{6}$$

where $\xi_0(T)$ is a Gaussian random variable of mean $\langle \xi_0(T) \rangle = 0$ and variance $\langle \xi_0(T) \xi_0(T') \rangle = 2D\delta(T - T')$. In order to define the random sources $\cos(2\omega t)\xi(t)$ and $\sin(2\omega t)\xi(t)$ over the slow time scale, we consider their correlations

$$\langle \cos(2\omega t) \xi(t) \cos(2\omega t') \xi(t') \rangle = \epsilon^2 \langle \cos^2(2\omega t) \rangle \langle \xi_1(T) \xi_1(T') \rangle \, , \tag{7}$$

$$\langle \sin(2\omega t) \xi(t) \sin(2\omega t') \xi(t') \rangle = \epsilon^2 \langle \sin^2(2\omega t) \rangle \langle \xi_2(T) \xi_2(T') \rangle \, , \tag{8}$$

where $\xi_1(T)$ and $\xi_2(T)$ are Gaussian random variables of mean $\langle \xi_j(T) \rangle = 0$ with $j = \{1, 2\}$ and correlation $\langle \xi_j(T)\xi_k(T') \rangle = 2D\delta(T - T')$ if $j = k$, and 0 otherwise. We further replace the average of the square of the oscillating functions in Eqs. (7) and (8) by their time averages over a period $\langle \cos^2(2\omega t) \rangle = \langle \sin^2(2\omega t) \rangle = 1/2$. The resulting random sources over the slow time scale are,

$$\cos(2\omega t)\xi(t) \to \frac{\epsilon}{\sqrt{2}}\xi_1(T) \ , \tag{9}$$

$$\sin(2\omega t)\xi(t) \to \frac{\epsilon}{\sqrt{2}}\xi_2(T) \ . \tag{10}$$

By substituting Eqs. (6), (9), and (10) into Eq. (5) we obtain a closed stochastic differential equation describing the slow temporal evolution of A,

$$\begin{aligned} \epsilon^3 \partial_T A(T) = \frac{1}{\omega} \Big\{ & \mu\epsilon A(T) + \nu\epsilon B(T) - \epsilon^3 \frac{b\omega}{4} A(T) \left[A^2(T) + B^2(T) \right] \\ & + \epsilon^2 B(T)\xi_0(T) - \frac{\epsilon^2}{\sqrt{2}} B(T)\xi_1(T) - \frac{\epsilon^2}{\sqrt{2}} A(T)\xi_2(T) \Big\} \ . \end{aligned} \tag{11}$$

The same procedure is repeated to determine the equation for the envelope variable $B(T)$. Multiply both sides of Eq. (4) by $L^{-1} \int_0^L dt \cos(\omega t)$, where $L = 2\pi/\omega$, and perform the integration. Together with Eqs. (6), (9), and (10), it leads to

$$\begin{aligned} \epsilon^3 \partial_T B(T) = \frac{1}{\omega} \Big\{ & -\nu\epsilon A(T) + \mu\epsilon B(T) - \epsilon^3 \frac{b\omega}{4} B(T)[A^2(T) + B^2(T)] \\ & - \epsilon^2 A(T)\xi_0(T) - \frac{\epsilon^2}{\sqrt{2}} A(T)\xi_1(T) + \frac{\epsilon^2}{\sqrt{2}} B(T)\xi_2(T) \Big\} \ . \end{aligned} \tag{12}$$

In matrix form, our final result for the Langevin equation for the envelopes is,

$$\begin{aligned} \frac{d}{dT} \begin{bmatrix} A \\ B \end{bmatrix} = & \frac{1}{\omega} \begin{bmatrix} \tilde{\mu} & \tilde{\nu} \\ -\tilde{\nu} & \tilde{\mu} \end{bmatrix} \begin{bmatrix} A \\ B \end{bmatrix} - \frac{b}{4} \begin{bmatrix} A\,(A^2 + B^2) \\ B\,(A^2 + B^2) \end{bmatrix} + \frac{1}{\epsilon\omega} \begin{bmatrix} 0 & 1 \\ -1 & 0 \end{bmatrix} \begin{bmatrix} A \\ B \end{bmatrix} \xi_0(T) \\ & + \frac{1}{\sqrt{2}\epsilon\omega} \left\{ \begin{bmatrix} 0 & -1 \\ -1 & 0 \end{bmatrix} \begin{bmatrix} A \\ B \end{bmatrix} \xi_1(T) + \begin{bmatrix} -1 & 0 \\ 0 & 1 \end{bmatrix} \begin{bmatrix} A \\ B \end{bmatrix} \xi_2(T) \right\} \ . \end{aligned} \tag{13}$$

We have also assumed the scaling $\mu = \epsilon^2\tilde{\mu}$ and $\nu = \epsilon^2\tilde{\nu}$ close to the bifurcation (to be verified

for consistency later). The Fokker-Planck equation associated to Eq. (13) is [19]

$$\begin{aligned}\frac{\partial}{\partial T}p(A,B,T) &= -\frac{1}{\omega}\frac{\partial}{\partial A}\left\{\left[\tilde{\mu}A+\tilde{\nu}B-\frac{1}{4}b\omega A(A^2+B^2)\right]p(A,B,T)\right\}\\ &-\frac{1}{\omega}\frac{\partial}{\partial B}\left\{\left[-\tilde{\nu}A+\tilde{\mu}B-\frac{1}{4}b\omega B(A^2+B^2)\right]p(A,B,T)\right\}\\ &+\frac{D}{\omega^2\epsilon^2}\left\{\left[A^2\frac{\partial^2}{\partial B^2}-2AB\frac{\partial^2}{\partial A\partial B}+B^2\frac{\partial^2}{\partial A^2}-\left(A\frac{\partial}{\partial A}+B\frac{\partial}{\partial B}\right)\right]p(A,B,T)\right\}\\ &+\frac{D}{2\omega^2\epsilon^2}\left\{\left[A^2\frac{\partial^2}{\partial B^2}+2AB\frac{\partial^2}{\partial A\partial B}+B^2\frac{\partial^2}{\partial A^2}+\left(A\frac{\partial}{\partial A}+B\frac{\partial}{\partial B}\right)\right]p(A,B,T)\right\}\\ &+\frac{D}{2\omega^2\epsilon^2}\left\{\left[A^2\frac{\partial^2}{\partial A^2}-2AB\frac{\partial^2}{\partial A\partial B}+B^2\frac{\partial^2}{\partial B^2}+\left(A\frac{\partial}{\partial A}+B\frac{\partial}{\partial B}\right)\right]p(A,B,T)\right\}\ ,\end{aligned} \tag{14}$$

We solve the equation order by order in ϵ. In order to find a stochastic contribution at lowest order, we assume $D=\epsilon^2\tilde{D}$. We also introduce polar coordinates $A=r\cos(\theta)$ and $B=r\sin(\theta)$. The probability distribution function in polar coordinates is $\tilde{p}(r,\theta,T)=rp(A,B,T)$, where r is the Jacobian of the transformation. In these variables, the diffusive terms of the Fokker-Planck equation [Eq. (14)] that are factors of $\tilde{D}/2\omega^2$ are

$$(A^2+B^2)\left(\frac{\partial^2}{\partial A^2}+\frac{\partial^2}{\partial B^2}\right)+2\left(A\frac{\partial}{\partial A}+B\frac{\partial}{\partial B}\right)=r^2\frac{\partial^2}{\partial r^2}+3r\frac{\partial}{\partial r}+\frac{\partial^2}{\partial\theta^2}\ , \tag{15}$$

whereas terms that are proportional to $\tilde{D}/\omega^2$ transform as

$$A^2\frac{\partial^2}{\partial B^2}-2AB\frac{\partial^2}{\partial A\partial B}+B^2\frac{\partial^2}{\partial A^2}-\left(A\frac{\partial}{\partial A}+B\frac{\partial}{\partial B}\right)=\frac{\partial^2}{\partial\theta^2}\ . \tag{16}$$

Furthermore, the drift terms of Eq. (14) are

$$\frac{\partial}{\partial A}\left[Ap(A,B,T)\right]+\frac{\partial}{\partial B}\left[Bp(A,B,T)\right]=\frac{1}{r}\frac{\partial}{\partial r}\left[r\tilde{p}(r,\theta,T)\right]\ , \tag{17}$$

$$\frac{\partial}{\partial A}\left[Bp(A,B,T)\right]-\frac{\partial}{\partial B}\left[Ap(A,B,T)\right]=-\frac{1}{r}\frac{\partial}{\partial\theta}\left[\tilde{p}(r,\theta,T)\right]\ , \tag{18}$$

$$\begin{aligned}\frac{\partial}{\partial A}\left\{\left[A(A^2+B^2)\right]p(A,B,T)\right\}+\frac{\partial}{\partial B}\left\{\left[B(A^2+B^2)\right]p(A,B,T)\right\}=\\ \frac{1}{r}\frac{\partial}{\partial r}\left[r^3\tilde{p}(r,\theta,T)\right]\ .\end{aligned} \tag{19}$$

Use also the following identity,

$$\left(r^2\frac{\partial^2}{\partial r^2}+3r\frac{\partial}{\partial r}\right)\frac{\tilde{p}(r,\theta,T)}{r}=\frac{1}{r}\left\{\frac{\partial^2}{\partial r^2}[r^2\tilde{p}(r,\theta,T)]-3\frac{\partial}{\partial r}[r\tilde{p}(r,\theta,T)]\right\}\ . \tag{20}$$

Combining Eqs. (15) and (16), together with Eqs. (17), (18), and (19), and by using Eq. (20), the Fokker-Planck equation in polar coordinate is then,

$$\begin{aligned}\frac{\partial}{\partial T}\tilde{p}(r,\theta,T) =& \frac{\tilde{\nu}}{\omega}\frac{\partial}{\partial\theta}\tilde{p}(r,\theta,T) + \frac{3\tilde{D}}{2\omega^2}\frac{\partial^2}{\partial\theta^2}\tilde{p}(r,\theta,T) \\ &- \frac{1}{\omega}\frac{\partial}{\partial r}\left[\left(\tilde{\mu}r - \frac{b\omega}{4}r^3\right)\tilde{p}(r,\theta,T)\right] \\ &+ \frac{\tilde{D}}{2\omega^2}\left\{\frac{\partial^2}{\partial r^2}[r^2\tilde{p}(r,\theta,T)] - 3\frac{\partial}{\partial r}[r\tilde{p}(r,\theta,T)]\right\} .\end{aligned} \tag{21}$$

We find that the radial and angular components of the Fokker-Planck equation [Eq. (21)] decouple. Let $\tilde{p}_s(r,\theta) = p_s(r)p_s(\theta)$. The stationary probability distribution function of the angular component satisfies $\partial_T p_s(\theta) = 0$ or

$$0 = \frac{\tilde{\nu}}{\omega}p_s(\theta) + \frac{3\tilde{D}}{2\omega^2}\frac{\partial}{\partial\theta}p_s(\theta) . \tag{22}$$

Integrating Eq. (22), the stationary probability distribution function of the angular component is

$$p_s(\theta) = \mathcal{N}_\theta e^{-\frac{2\omega}{3\tilde{D}}\tilde{\nu}\theta} , \tag{23}$$

where $\mathcal{N}_\theta$ is a normalization constant. Furthermore, the stationary probability distribution function of the radial component satisfies $\partial_T p_s(r) = 0$ or

$$0 = -\frac{1}{\omega}\left(\tilde{\mu}r - \frac{b\omega}{4}r^3\right)p_s(r) + \frac{\tilde{D}}{2\omega^2}\left\{\frac{\partial}{\partial r}[r^2 p_s(r)] - 3rp_s(r)\right\} . \tag{24}$$

Integrating Eq. (24), the stationary probability distribution function of the radial component is

$$p_s(r) = \mathcal{N}_r r^{\frac{2\omega\tilde{\mu}}{\tilde{D}}+1}e^{-\frac{b\omega^2}{4\tilde{D}}r^2} , \tag{25}$$

where $\mathcal{N}_r$ is a normalization constant. The stationary probability distribution function is normalized so that

$$1 = \int_0^{2\pi}\int_0^{\infty}\tilde{p}_s(r,\theta)drd\theta = \left[\int_0^{2\pi}p_s(\theta)d\theta\right]\left[\int_0^{\infty}p_s(r)dr\right] , \tag{26}$$

and we choose to normalize both terms in square brackets of Eq. (26) to one. The normalization constant of the stationary probability distribution function of the angular component is

$$\mathcal{N}_\theta = \left(\frac{\tilde{\nu}\omega}{3\tilde{D}}\right)\frac{e^{\frac{2\pi\tilde{\nu}\omega}{3\tilde{D}}}}{\sinh(\frac{2\pi\tilde{\nu}\omega}{3\tilde{D}})} . \tag{27}$$

The bifurcation threshold is located at the point where $p_s(\theta)$ is constant. This occurs at $\tilde{\nu} = 0$ where $p_s(\theta) = 1/(2\pi)$. Furthermore, the normalization constant of the stationary probability distribution function of the radial component is

$$\mathcal{N}_r = 2\left(\frac{4\tilde{D}}{b\omega^2}\right)^{-\left(\frac{\alpha+1}{2}\right)} \Gamma^{-1}\left(\frac{\alpha+1}{2}\right) , \tag{28}$$

where the exponent of the power law in Eq. (25) is

$$\alpha = \frac{2\omega\tilde{\mu}}{\tilde{D}} + 1 . \tag{29}$$

If $\alpha < -1$, the probability distribution function is negative which is unphysical. We then define the location of the threshold as the point where the exponent of the power law is -1. We obtain as a result two conditions at threshold,

$$\nu = \omega^2 - \omega_0^2 - \eta\cos(\omega\tau) + \omega\kappa\sin(\omega\tau) = 0 , \tag{30}$$

$$\mu\omega + D = \beta\omega^2 + \eta\omega\sin(\omega\tau) + \omega^2\kappa\cos(\omega\tau) + D = 0 . \tag{31}$$

Equations (30) and (31) validate the consistency of the assumption about the scaling of the parameters μ, ν, and D close to the bifurcation. These conditions can be further reduced by expanding Eqs. (30) and (31) up to order τ. One obtains the Hopf frequency from Eq. (30),

$$\omega = \sqrt{\frac{\omega_0^2 + \eta}{1 + \kappa\tau}} . \tag{32}$$

Furthermore, the exponent of the power law in the expression for the radial component of the probability distribution function is

$$\alpha = \frac{2}{D}\left(\frac{\omega_0^2 + \eta}{1 + \kappa\tau}\right)(\beta + \eta\tau + \kappa) + 1 . \tag{33}$$

We finally define the location of the bifurcation threshold as $\alpha_c = -1$, or

$$(\omega_0^2 + \eta)(\beta + \eta\tau + \kappa) = -D(1 + \kappa\tau) . \tag{34}$$

We note that this result reduces when $\tau = 0$ to that given by Lücke [8] and Drolet and Viñals [9]. However, it disagrees with the results of Mayol et al. [13] by a numerical factor.

III. NUMERICAL ANALYSIS

We describe here a direct numerical integration of the model to validate the asymptotic expansion just described. We use the first order algorithm described in [20]. By defining $y(t) = \dot{x}(t)$, the numerical solution of Eq. (1) requires the following iteration

$$x(t+\Delta t) = x(t) + y(t)\Delta t \ , \tag{35}$$

$$y(t+\Delta t) = y(t) + \left[-\omega_0^2 x(t) - \eta x(t-\tau) + \beta y(t) + \kappa y(t-\tau) - b x^2(t) y(t)\right] \Delta t + x(t)\xi(t) \ , \tag{36}$$

where $\xi(t) = \sqrt{2D\Delta t}\psi_1(t)$, with $\psi_1(t)$ a random variable normally distributed with mean 0 and variance 1. We choose as initial condition in $[-\tau, 0]$ a random constant drawn from a Gaussian distribution also of mean 0 and variance 1. The equations are typically integrated up to $t_{max} = 500$, where the solution is believed to have reached a stationary state, by using an integration step of $\Delta t = 0.001$. The stationary probability density $p(x)$ is then constructed in the time interval $[t_{max}, t_{max} + 10]$. The overall process is repeated in order to generate an ensemble average of 10^6 independent trajectories. A phase portrait showing the velocity y and the position x of the deterministic delayed oscillator is shown in Fig. 1 for different values of the damping parameter β.

Our results for the stationary probability density are shown in Fig. 2. Below the bifurcation threshold ($\beta < \beta_c$), the stationary distribution if given by $p(x) = \delta(x)$. As expected ([16]), we observe instead a very long transient with $p(x)$ approximately a power law distribution with an apparent exponent $\alpha < -1$ at small x. This is a non-normalizable distribution and hence unphysical. It only appears as a long-lived transient. The probability amplitude at $x = 0$ (not shown in the figure) grows with time, signaling the build up of a delta function distribution. Because of normalization, the growth at $x = 0$ implies a decaying amplitude for $x > 0$ as shown in the figure. For $\beta > \beta_c$, we do obtain a time-independent power law distribution function with exponent $-1 < \alpha < 0$. This probability distribution function is normalizable and is the stationary distribution above threshold. We finally show $p(x)$ in the range of β values where it is bimodal.

The exponent α is estimated in the interval $x = \{0.01, 0.1\}$. Figure 3 shows the value of the exponent α obtained from a power law fit to $p(x)$ as a function of β. Predictions from Eq. (33) are also included for comparison. We observe a smooth variation of α with

β, allowing a convenient determination of β_c, the value for which $\alpha = -1$. That method was used to determine the threshold results shown in Figure 4. For sufficiently small values of the time delay τ ($\tau < 0.15$ for the set of parameters shown in the figure), the numerical results are found to be in excellent agreement with predictions from Eq. (34).

Finally, we have numerically computed the Hopf frequency close to the bifurcation threshold of the oscillator. The Hopf frequency corresponds to the frequency at which the amplitude of the Fourier transform of the trajectories is maximum. Our numerical results are shown in Fig. 5 as a function of the time delay, and compared to the analytic result Eq. (32). Once again, excellent agreement between the two sets of data is found provided the time delay is sufficiently small.

Acknowledgments

This research has been supported by NSERC Canada. We thank two Compute Canada sites: CLUMEQ and SciNet for access to supercomputing resources. Compute Canada is supported by the Canada Foundation for Innovation.

---

[1] E. V. Appleton and B. van der Pol, Phil. Mag. **43**, 177 (1922).

[2] A. Maccari, Nonlinear Dyn. **26**, 105 (2001).

[3] A. Maccari, Int. J. Nonlinear Mech. **38**, 123 (2003).

[4] A. Maccari, Phys. Scr. **76**, 526 (2007).

[5] J. Xu and K. W. Chung, Physica D **180**, 17 (2003).

[6] J. C. Ji and C. H. Hansen, Chaos Soliton Fract. **28**, 555 (2006).

[7] X. Li, J. C. Ji, C. H. Hansen, and C. Tan, J. Sound Vibrat. **291**, 644 (2006).

[8] M. Lücke, in *Theory of noise induced processes in special applications*, edited by F. Moss and P. McClintock (Cmabridge University Press, Cambridge, England, 1989).

[9] F. Drolet and J. Viñals, Phys. Rev. E **57**, 5036 (1998).

[10] P. H. Baxendale, in *IUTAM Symposium on Nonlinear Stochastic Dynamics*, edited by N. S. Namachchivaya and Y. K. Lin (Kluwer Academic Publishers, Dordrecht, The Netherlands, 2003), p. 492.

[11] R. Kuske, in *IUTAM Symposium on Nonlinear Stochastic Dynamics*, edited by N. S. Namachchivaya and Y. Lin (Kluwer Academic Publishers, Dordrecht, The Netherlands, 2003), p. 492.

[12] P. H. Baxendale, Stoch. Proc. Appl. **113**, 235 (2004).

[13] C. Mayol, R. Toral, and C. R. Mirasso, Phys. Rev. E. **69**, 066141 (2004).

[14] M. M. Klosek, Acta Phys. Pol. B **35**, 1387 (2004).

[15] M. M. Klosek and R. Kuske, Multiscale Model. Simul. **3**, 706 (2005).

[16] M. Gaudreault, F. Drolet, and J. Viñals, Phys. Rev. E **82**, 051124 (2010).

[17] K. A. Wisenfeld and E. Knobloch, Phys. Rev. A **26**, 2946 (1982).

[18] S. H. Strogatz, *Nonlinear dynamics and chaos : with applications to physics, biology, chemistry and engineering* (Addison-Wesley, MA, 1994).

[19] C. W. Gardiner, *Handbook of Stochastic Methods for Physics, Chemistry and the Natural Sciences* (Springer-Verlag, Berlin, 1997), 2nd ed.

[20] J. M. Sancho, M. San Miguel, S. L. Katz, and J. D. Gunton, Phys, Rev. A **26**, 1589 (1982).

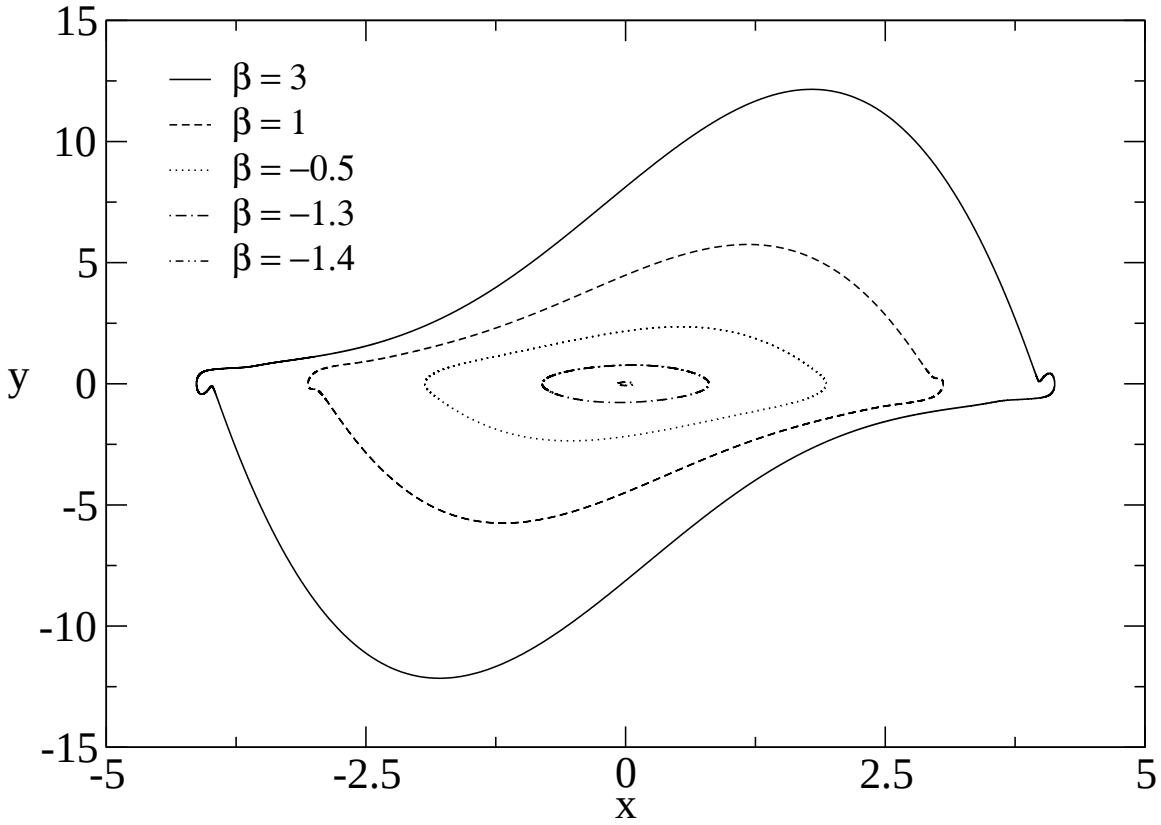

FIG. 1: Phase portrait of the deterministic ($D = 0$) van der Pol oscillator with delayed feedback for different values of the damping parameter β. The parameters are fixed at $\omega_0 = 1$, $b = 1$, $\eta = 1$, $\kappa = 1$, and $\tau = 1$.

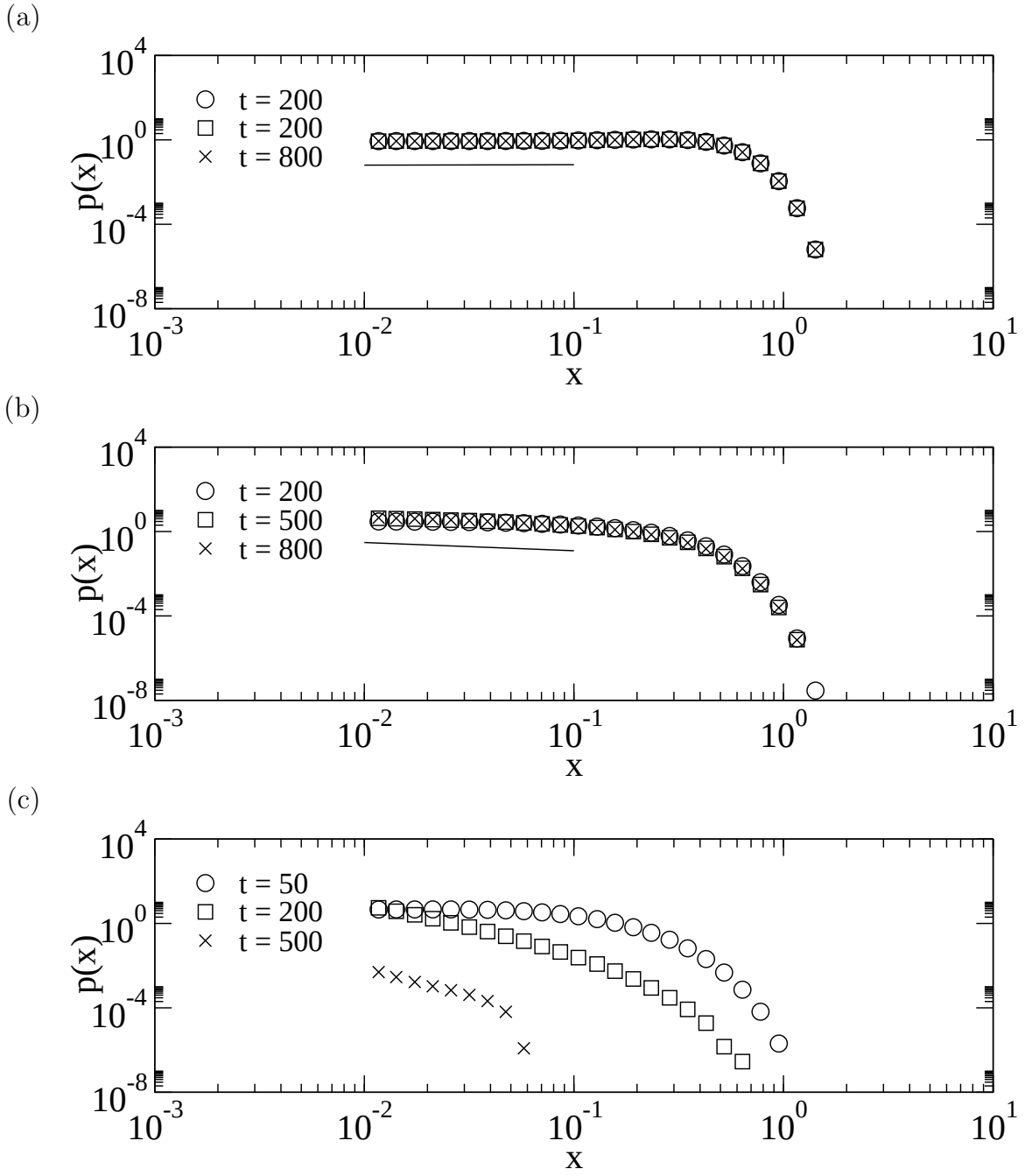

FIG. 2: Numerical determination of the stationary probability distribution function $p(x)$ as a function of the position x of the stochastic van der Pol oscillator with delayed feedback for which the upper bound t of the time window used to calculate the probability density is varied. The parameters are fixed at $\omega_0 = 1$, $\eta = 1$, $b = 1$, $\kappa = 1$, $\tau = 0.025$, and $D = 0.1$. The bifurcation is located at $\beta_c \simeq -1.08$ for this set of parameters. The distribution is stationary in (a) and (b) where $\alpha \simeq 0.02$ ($\beta = -1$) and $\alpha \simeq -0.39$ ($\beta = -1.04$) respectively. However, the probability density is no more stationary below threshold, as shown in (c) ($\beta = -1.1$). The solid line extends the domain used for the determination of the exponent.

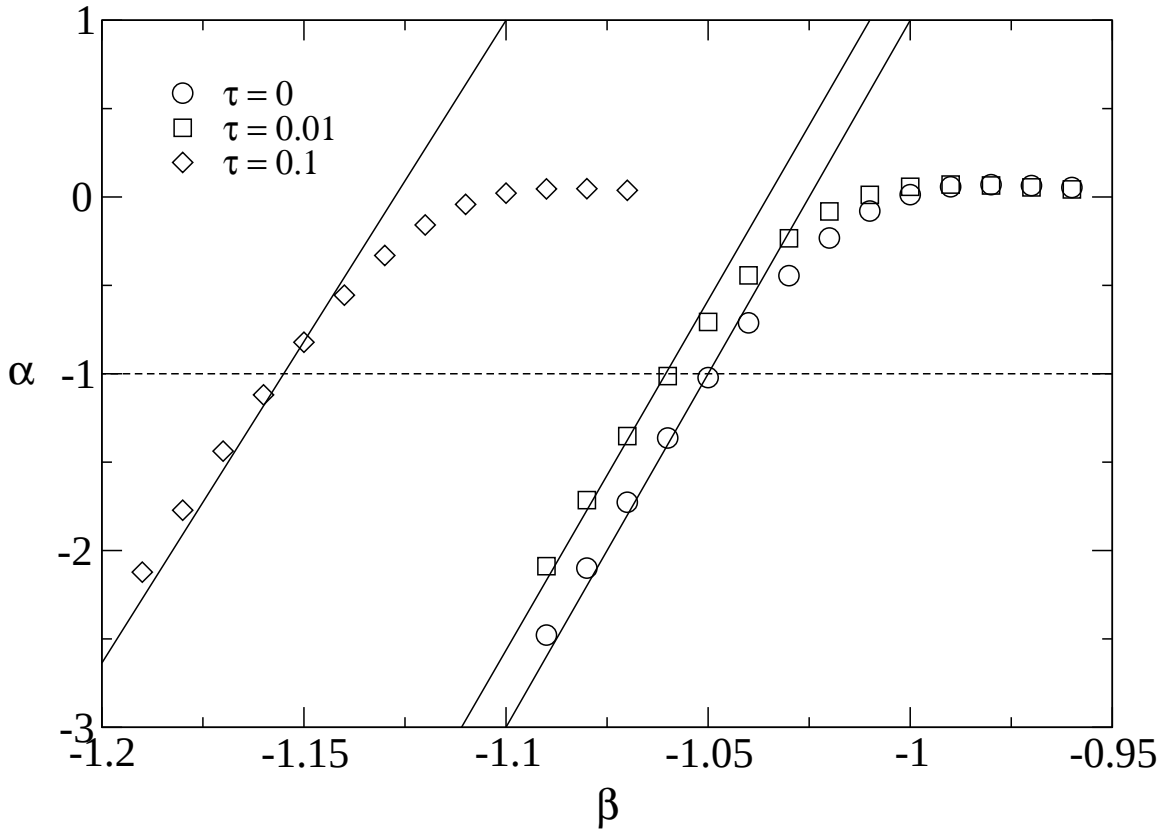

FIG. 3: Exponent of the power law α as a function of the damping parameter β calculated from the stationary probability distribution function $p(x)$ for the stochastic van der Pol oscillator with delayed feedback. The parameters are fixed at $\omega_0 = 1$, $\eta = 1$, $b = 1$, $\kappa = 1$, and $D = 0.1$. The calculations are done for three values of the time delay τ. The bifurcation point is located at $\alpha = -1$, point at which the distribution function becomes non-normalizable. The symbols are the results of the numerical simulations whereas the solid lines are the theoretical predictions from Eq. (33).

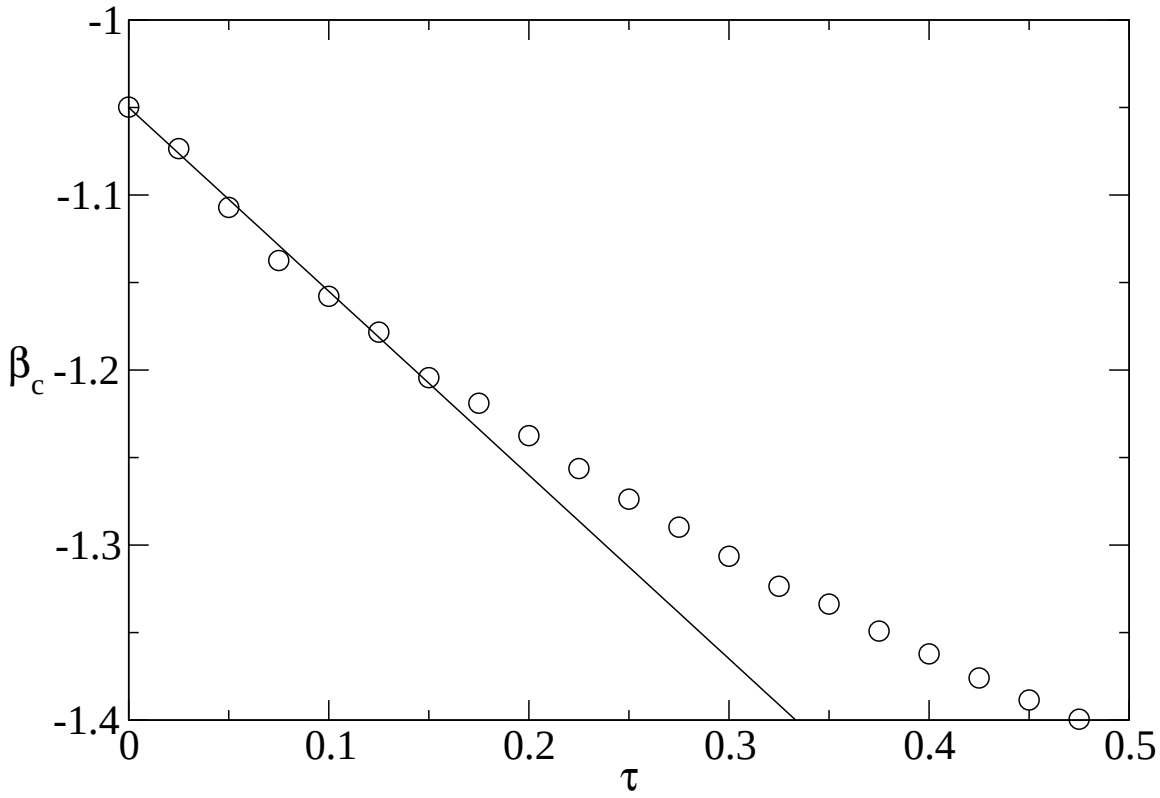

FIG. 4: Bifurcation diagram of Eq. (1). We show the parameter β_c evaluated at threshold as a function of the time delay τ. The parameters are fixed at $\omega_0 = 1$, $\eta = 1$, $b = 1$, $\kappa = 1$, and $D = 0.1$. The symbols are the numerically determined threshold calculated as the point for which the exponent of the power law of the stationary probability distribution function is -1 whereas the solid curve corresponds to Eq. (34). The agreement between the two is excellent when the time delay is small.

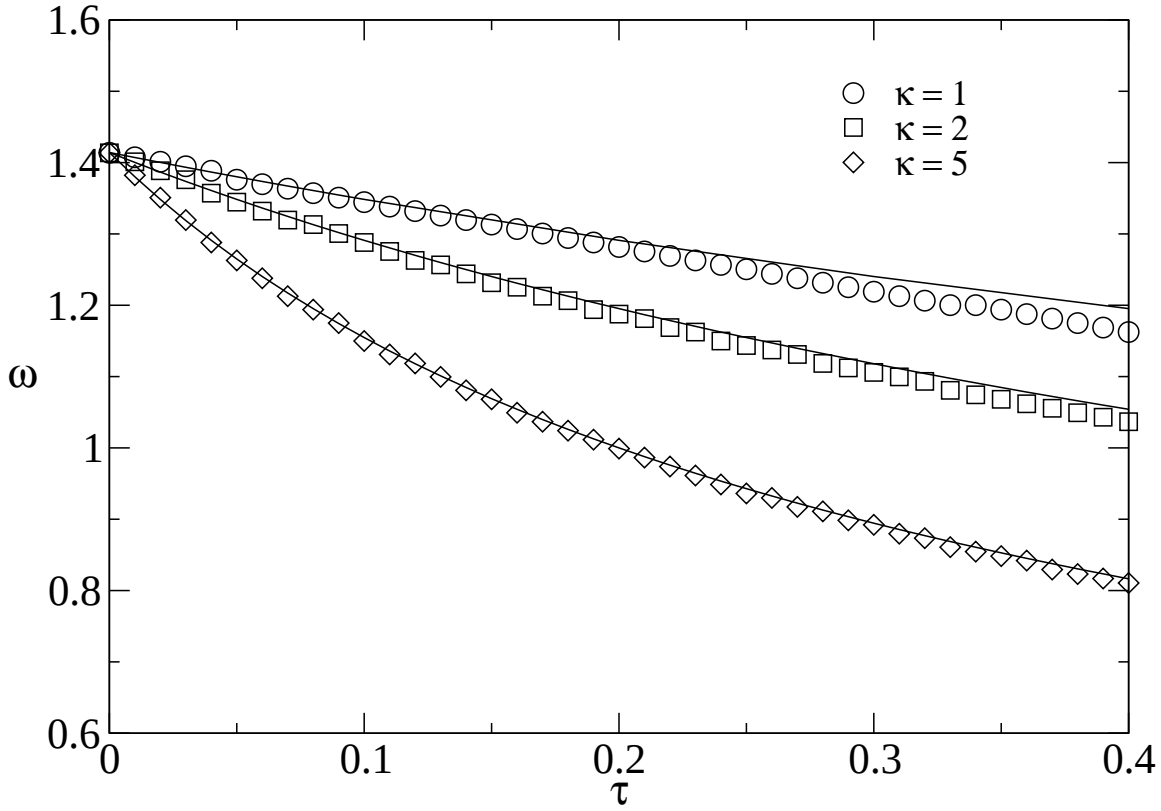

FIG. 5: Frequency ω of the oscillation as a function of the time delay τ for different values of the intensity of the delayed velocity κ. The parameters are fixed at $\omega_0 = 1$, $\eta = 1$, $b = 1$, and $D = 0.1$. The damping parameter is chosen to be close and below the bifurcation $\beta = -\kappa$. The symbols are the numerically determined frequency whereas the solid curve is Eq. (32).